CHARACTERIZATION OF FIBROSIS AND HYPERTROPHY IN A FELINE MODEL OF HFpEF

A Thesis
Submitted to
the Temple University Graduate Board

In Partial Fulfillment
of the Requirements for the Degree
MASTER OF BIOMEDICAL SCIENCES

---

by
Deborah M. Eaton
May 2018

Thesis Approvals:

Steven R. Houser, PhD, Cardiovascular Research Center
Meredith Brisco-Bacik, MD, Department of Cardiology
Walter J. Koch, PhD, Center for Translational Medicine
Marla R. Wolfson, MS, PhD, Departments of Physiology, Thoracic Medicine and Surgery
Sadia Mohsin, PhD, Cardiovascular Research Center

ABSTRACT

Rationale: Heart failure with preserved ejection fraction (HFpEF) is rapidly growing as a major public health problem and there are no proven therapeutics available. This lack of therapeutics may be partially attributed to the lack of well-established animal models and understanding of the underlying pathophysiology.

Aim: Our aim was to complete an in-depth fibrotic and hypertrophy analysis of the feline HFpEF heart.

Methods and Results: Male kittens, age 2 months, underwent aortic banding to induce a slow, progressive pressure overload resulting in a HFpEF phenotype. Four months after banding, terminal studies were conducted after which the heart was explanted and underwent a histological work up. The fibrotic area was examined using Masson's trichrome staining and cardiomyocyte cross-sectional area was examined by staining for the cell membrane. There was a significant increase in left ventricle fibrosis in banded cats compared to sham animals. In banded cats, the sub-endocardial layer of the left ventricle had more fibrosis than the sub-epicardial layer of the left ventricle. There was an increase in fibrosis in the left atrium, right atrium, and right ventricle in the banded animals compared to the sham animals, but it did not reach statistical significance. There was a significant increase in the cardiomyocyte cross-sectional area of banded cats compared to sham cats.

Conclusions: An in-depth analysis of the feline HFpEF heart revealed important insights into the state of fibrosis and hypertrophy, which further supports the use of this model as pre-clinical platform for testing therapeutics.

ACKNOWLEDGEMENTS

First, I must thank Dr. Steven Houser for the chance to join his lab, work on this project, and giving me every opportunity possible. I had no idea what was in store for me at Temple, but none of it would have been possible without his support and guidance. This has been a once in a life time opportunity and Dr. Houser will continue to be a guiding force for me. His career is legendary and the passion he has for his work is incredible to see first-hand.

To the other members of my committee, Dr. Walter Koch, Dr. Meredith Brisco-Bacik, and Dr. Marla Wolfson, thank you so much for helping to shape my project and providing invaluable feedback. I couldn't have asked for a better group of experts and still can't believe that I had the privilege to learn from each of you. I also really appreciate Dr. Sadia Mohsin taking the time to attend my defense as the additional committee member.

I want to thank the rest of the Houser lab for creating such a great work environment. I look forward to coming in every day because of the amazing people I'm surrounded by. Everyone has made me feel at home from the moment I started and I wouldn't have been able to complete my project without everyone's help.

I must thank Remus Berretta for teaching me so much the past two years. Every day in the EDIF was a new lesson, and I'm so glad I had the chance to gain some insight and new jokes from his 20+ years of experience.

My interest in cardiovascular science was jump started by Dr. Beth Bailey when I was a freshman in college, and almost six years later I can't imagine life without research. She believed in me even when I didn't believe in myself and pushed (forced) me to be independent, even when I resisted the teaching moments.

To my mom and the rest of my family, I wouldn't have made it here without you. Any steps forward I take are only possible because I know I have your support.

Lastly, I want to thank Dr. Markus Wallner. I remember the first time I tagged along for echo and over a year later, here we are. He has been my biggest inspiration and I could not have asked for a better teacher. As I move forward in my career, I hope to hold myself to the same high standards and commitment to excellence that he has modeled for me. I wouldn't have grown so much as a person without his input, guidance, and life lessons over the last year and a half. Vielen Dank!

TABLE OF CONTENTS

LIST OF TABLES

LIST OF FIGURES

Figure Page

ABBREVIATIONS

HFpEF: Heart Failure with Preserved Ejection Fraction

HFrEF: Heart Failire with Reduced Ejection Fraction

CSA: Cross-sectional area

ECHO: Echocardiography

ESC: European Society of Cardiologists

PH: Pulmonary Hypertension

LVEDP: Left ventricular end-diastolic pressure

NTpro-BNP: N-terminal pro b-type natriuretic peptide

LV FS: Left Ventricle Fractional Shortening

LV: Left Ventricle

LVS: Left Ventricle Septal Wall

LVL: Left Ventricle Lateral Wall

RA: Right Atrium

LA: Left Atrium

RV: Right Ventricle

LAV_{ES}: Left Atrium End Systolic Volume

FFR: Fractional Flow Reserve

HW: Heart Weight

BW: Body Weight

DAPI: 4',6-diamidino-2-phenylindol

BNP: Brain natriuretic peptide

WGA: Wheat Germ Agglutin

CHAPTER 1

INTRODUCTION

Significance

Heart failure is defined by the American Heart Association as a "chronic, progressive condition in which the heart muscle is unable to pump enough to meet the bodies needs for blood and oxygen" [1]. Heart failure is a major public health concern and only seems to be growing in the number of patients impacted. There are 5.7 million adults living with heart failure in the United States, and this number is only expected to rise in the future, exceeding 8 million people by 2030[2]. The estimated financial burden of heart failure is $30.7 billion per year in the United States alone. Approximately $21 billion is direct costs, while $10 billion is indirect costs[3]. However, there is also a large international financial burden as well. The overall direct costs internationally are $65 billion per year and indirect costs are estimated to be $43 billion per year [4]. With such high financial burdens associated with the disease, a better understanding of the underlying pathophysiology and better treatments are urgently needed.

Heart Failure Background

There are three main classifications of heart failure; heart failure with reduced ejection fraction (HFrEF), heart failure with mid-range ejection fraction (HFmEF), and heart failure with preserved ejection fraction (HFpEF). The American Heart Association defines ejection fraction as "a percent measurement of how much blood the left ventricle pumps out with each contraction"[1]. Around half of heart failure patients are diagnosed with HFpEF, while the other half are diagnosed with HFrEF [5]. However, there is a group of patients who fall in between which is defined as HFmEF [6]. HFrEF is associated with more

severely reduced systolic function and an ejection fraction less than 40%, while HFpEF is associated with moderately reduced systolic function and an ejection fraction greater than 50% [7].

The classification of HFmEF was termed out of necessity for the group of patients who had ejection fractions that fell between the reduced ejection fraction of 40% and preserved ejection fraction greater than 50%. The prevalence of HFmEF has been estimated to be 10-20% based off data collected from clinical studies [8]. The mortality rate of HFmEF was documented as 115 deaths per 1,000 people per year [8]. Phenotypically HFmEF has been described as having left ventricle eccentric remodeling in between HFpEF and HFrEF, decreased left ventricle contractility, increased left ventricle diastolic stiffness closer to what is seen in HFpEF patients [8].

HFpEF Background

The term HFpEF is relatively new. In the 1970-80's, patients were diagnosed with diastolic dysfunction or diastolic heart failure [9]. Overtime it became more clear that diastolic dysfunction was a homogenous term being applied to a non-homogenous patient population[10]. Just because one set of patients had normal systolic function with compromised diastolic function, did not mean that a different set of patients with compromised diastolic function could not have reduced systolic function. For a brief period of time, it was referred to as diastolic heart failure or heart failure with normal ejection fraction[11]. Overtime as the cardiology field has evolved, HFpEF has become the accepted term and widely used[12]. The European Society of Cardiology defines HFpEF as having the signs and symptoms of HF, LVEF $\geq$ 50%, elevated levels of natriuretic peptides

(BNP>35pg/ml and/or NT-proBNP>125pg/ml), and at least one of the following: left ventricle hypertrophy, left atrium enlargement, diastolic dysfunction [6].

Patients diagnosed with HFpEF are more likely to be female and older in age compared to HFrEF patients [13]. Approximately 50% of HFpEF patients have five or more comorbidities, which can be either cardiac or non-cardiac specific [14]. The cardiac specific comorbidities include: atrial fibrillation, systolic LV dysfunction, ventricular-vascular stiffening, impaired systemic vasodilatory reserve, chronotropic incompetence, pulmonary hypertension, RV dysfunction[15]. Non-cardiovascular specific comorbidities include: obesity, diabetes mellitus, metabolic syndrome, hypertension, renal dysfunction, chronic obstructive pulmonary disease, and anemia[13, 15]. Many of these comorbidities are associated with a chronic state of inflammation, which may play a role in disease progression [16].

HFpEF Clinical Trials

While there are multiple treatment options available for HFrEF, clinical trials focused on HFpEF have not produced positive results. Therapies such as angiotensin-converting enzyme (ACE) inhibitors, angiotensin receptor blocker (ARB), and β-blockers did not have a beneficial effects on HFpEF patient's prognosis [17] (Table 1). This may be partially explained by the lack of understanding regarding the underlying pathophysiology leading to HFpEF.

Table 1. Completed HFpEF Clinical Trials. Source: Clinical Trials Database, National Institute of Health [18].

Trial Name	Therapeutic	Ending Phase	Primary Completion Date
Reduced Contractile Reserve: a Therapeutic Target in Heart Failure With Preserved Ejection Fraction(HFpEF)	Dobutamine Amlodipine	Completed	December 2013
Acute Effects of Inorganic Nitrite on Cardiovascular Hemodynamics in Heart Failure With Preserved Ejection Fraction	Nitrine	Completed	October 2014
Pilot Feasibility Study of the Safety and Efficacy of Anakinra in Heart Failure with Preserved Ejection Fraction	Anakinra	Completed	June 2013
Inhaled Sodium Nitrite on Heart Failure With Preserved Ejection Fraction	Sodium Nitrite Inhalation Solution	Completed	December 2015
Nitrate's Effect on Activity Tolerance in Heart Failure With Preserved Ejection Fraction (NEAT-HFpeF)	Isosorbide Mononitrate	Completed	February 2015
Perhexiline Therapy in Heart Failure With Preserved Ejection Fraction Syndrome	Perhexiline	Completed	February 2014
A Study to Evaluate the Effects of 4 Weeks Treatment With Subcutaneous Elamipretide on Left Ventricular Function in Subjects With Stable Heart Failure With Preserved Ejection Fraction	Elamipretide	Completed	May 2017
Sildenafil in HFpEF (Heart Failure With Preserved Ejection Fraction) and PH	Sildenafil	Completed	September 2014
Evaluation of Enalapril Versus Placebo in Patients With Diastolic Heart Failure (PIE-I)	Enalapril	Completed	June 2004
Ranolazine in Diastolic Heart Failure (RALI-DHF)	Ranolazine	Completed	February 2011
Phase IIb Safety and Efficacy Study of Four Dose Regimens of BAY1021189 in Patients With Heart Failure and Preserved Ejection Fraction Suffering From Worsening Chronic Heart Failure (SOCRATES-PRESERVED)	Vericiguat	Completed	August 2015
Physiological Effects of Grape Seed Extract in Diastolic Heart Failure (GRAPEVINE-HF)	Grape Seed Extract	Completed	November 2013
Anemia in Heart Failure With a Preserved Ejection Fraction (HFPEF)	Erythropoietin alpha	Completed	November 2012
LCZ696 Compared to Valsartan in Patients With Chronic Heart Failure and Preserved Left-ventricular Ejection Fraction	Valsartan	Completed	December 2011
Aldosterone Antagonist Therapy for Adults With Heart Failure and Preserved Systolic Function (TOPCAT)	Spironolactone	Completed	June 2013
Safety and Efficacy Trial to Treat Diastolic Heart Failure Using Ambrisentan	Ambrisentan	Terminated	September 2013

Pathophysiology associated with HFpEF

A healthy left ventricle has two main functions. It must be compliant in order to fill the ventricle during diastole at acceptable low pressures, and it must be firm enough to eject the stroke volume during systole [19]. The changes that are occurring in the heart leading to diastolic dysfunction include an increase in myocardial stiffness and myocardial inactivation, which occurs as a result of contractile myofilaments breaking apart and

calcium reuptake to the sarcoplasmic reticulum[20]. Concentric hypertrophy is observed during HFpEF, which means that the walls of the ventricles are becoming thicker without changing the internal chamber dimensions, but can eventually lead to a reduction in chamber dimensions [13]. The myocytes undergo morphological changes, becoming thicker, shorter and sarcomeres are added in parallel[21]. There is also an increase in the collagen content, but not a loss in the number of myocytes [22, 23]. These changes are detrimental to cardiac function.

Cardiac Remodeling

A key determinant in myocardial stiffness is the extracellular matrix, more specifically collagen [20]. Collagen synthesis, post-synthetic processing, post-translational modification and degradation are all essential in maintaining normal collagen levels [24]. It has been established that in HFpEF the net increase in collagen is the product of an increase in collagen synthesis, and a decrease in collagen degradation, which ultimately results in the presence of reactive, interstitial fibrosis [25]. Fibrosis is associated with many different mechanisms of impairing heart function, including decreased compliance, impaired oxygen diffusion and electrical activity due to repolarization problems [26, 27]. A four stage process has been proposed for the development of fibrosis: 1. Initiation of response due to injury, or in terms of this project progressive pressure overload, 2. Activation of effector cells, 3. Growth of the extracellular matrix, and 4. Imbalance of the growth and break down of the extracellular matrix [27]. The heart is not alone in the development of fibrosis; some of the factors are common across organs. An increase in transforming growth factor beta (TGF- β) plays a major role as a molecular initiator for both the development of fibrosis and hypertrophy [27, 28]. The effector cells responsible for cardiac fibrosis are cardiac

fibroblasts. Sources of cardiac fibroblasts include myocardial fibroblasts, circulating fibroblasts, epithelial-to-mesenchymal transitioned fibroblasts, and even collagen-secreting bone marrow-derived cells [26, 27]. Once the fibrotic pathway is initiated, the formation of myofibroblasts is pushed forward by TGF-β1, endothelin-1, and angiotensin II [27] (Figure 1).

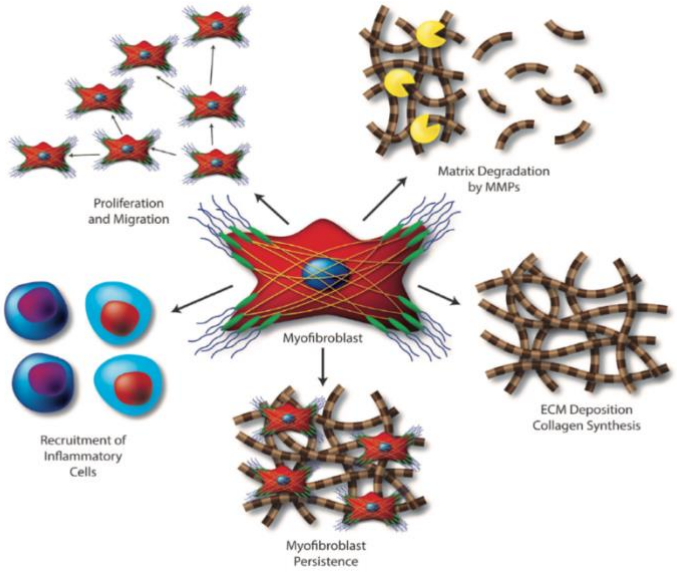

Figure 1. Role of Myofibroblasts in Development of Fibrosis
Myofibroblasts play an important role in the development of fibrosis and the overall decrease in cardiac function. Myofibroblasts propagate the inflammatory state, degradation of matrix, ECM deposition and collagen formation, and even more myofibroblast development. ECM = extracellular matrix. Used with permission (Travers, 2016).

The healthy structure of the heart is a complex network of muscle working together to meet the demands of the body. Collagen provides support to the cardiomyocytes via the extracellular matrix and has different sub-types to fit the various functions needed. Type I collagen consists of thick parallel fibrils that play a role in providing high tensile strength, and account for approximately 85% of the fibrous collagen present in the heart [29, 30]. Type III collagen is composed much more of fine fibrils compared to Type I collagen, and is

important in maintaining the elastic nature of the matrix [29]. There are fibrous elastic tissue envelopes around the heart as a whole, around and between cardiomyocytes. The epimysium is on the outside of endocardial and epicardial surfaces and surrounds the heart as a whole [29]. Cardiomyocytes are surrounded and connected by perimysium sheaths. Single cardiomyocytes themselves are surrounded by endomysium sheaths.

It is well established that cardiac hypertrophy is how the heart responds to both pressure and volume overload [21]. When the heart is in a hypertrophic state, embryonic gene expression is increased, ie. natriuretic peptides and fetal contractile peptides[31, 32]. Biomechanical sensors, which includes myocytes and non-myocyte cells, "monitor" the hemodynamic load and when an increase in pressure occurs, growth factors and cytokines produce growth factors, resulting in a very localized response to the area where the pressure overload was sensed [32]. G protein-coupled receptors are thought to be activated by "endothelin-1, angiotensin II, interleukin-6-related cyotkines" and receptor tyrosine kinases are thought to be activated by insulin-like growth factor[32]. These factors and their receptors on the cell-surface are the initial step in myocyte growth and progression of hypertrophy.

A common biomarker used to track the progression of heart failure and classify patient's progression is B-type natriuretic peptide (BNP). Normally, natriuretic peptides are important in stabilizing blood pressure and regulating salt and water balance in order to maintain blood volume[33]. However, cardiomyocytes secrete BNP in response to stretch and is secreted from both the atria and ventricles [34, 35]. Increased BNP levels act as an important alarm that abnormal changes may be occurring in the heart. BNP and NT-proBNP, which is the N-terminal pro-hormone of BNP, can be measured in the circulation.

However, laboratory tests that are commonly available focus on measuring levels of NT-proBNP[35].

We have established a feline model of HFpEF using customized pre-shaped bands around the aorta of two-month old kittens, which results in a slow, progressive pressure overload as the animals mature[36]. This model will be used for pre-clinical testing of therapeutics and provides a great variety of functional data through echocardiography and invasive hemodynamics. Parameters such as left ventricle end diastolic pressure, dp/dt max, dp/dt min, cardiac output, mean pulmonary arterial pressure, left ventricle fractional shortening, left atrium end systolic volume, and left atrium ejection fraction are all extremely useful for evaluating animals at 4 months post-banding and provide many different measurements for evaluating the efficacy of therapies. However, it is also important to understand the morphological changes that are occurring in the heart during a disease state. The left ventricle dysfunction characteristic of HFpEF is thought to be induced by cellular hypertrophy, interstitial fibrosis or a combination of both pathologies [37]. Fibrosis is therefore a potential target for treating HFpEF. In order to understand the impact of therapeutics on the fibrosis, having a baseline characterization of the fibrosis and cardiomyocyte hypertrophy present during HFpEF is necessary.

CHAPTER 2

METHODS

Aortic Banding Procedure

All animal procedures were approved by the Temple University Lewis Katz School of Medicine Institutional Animal Care and Use Committee. Following baseline measurements (ECHO, blood collection and pulmonary function testing), male two-month-old kittens underwent a mini-thoracotomy during which the animal underwent either the aortic banding procedure with a customized, pre-shaped band or a sham operation as previously described [38-41] (Figure 2). A pre-shaped band was put in place around ascending aorta proximal of the outgoing branches and gently tied down to avoid immediate constriction. This step of the procedure is extremely important because if the band is tied down too tightly and causes an immediate pressure overload, the animal will develop left ventricle dilation and therefore presents a different phenotype.

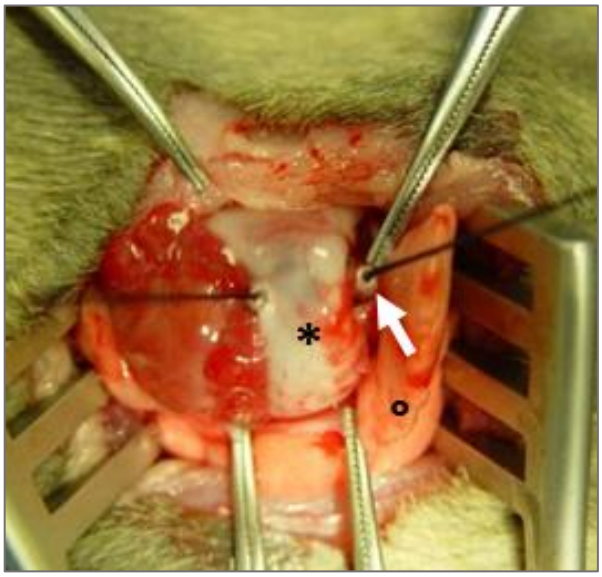

Figure 2. Aortic Banding Surgery
Mini thoracotomy with lungs (°) and the pre-shaped band (white arrow) placed around the aorta.

Post-surgery Maturation Period

Animals were monitored for four months post-banding as they matured. During this time, the animals were group housed and able to roam freely. They underwent monthly serial blood draws, echocardiograms and pulmonary function tests. Four months post-banding animals underwent terminal invasive hemodynamic procedures.

NTpro-BNP

Arterial blood, collected via cephalic vein puncture at baseline and 4 months post-banding, was stored in EDTA vacutainers and centrifuged at 1300rpm for 15 minutes. The plasma was then separated from the rest of the blood sample and sent to Idexx Laboratories (Memphis, TN) to measure NT-proBNP levels via ELISA.

Tissue Harvesting and Processing

After the completion of the terminal studies, an extensive tissue harvest protocol was carried out. Lung, diaphragm, kidney, soleus, and liver were all harvested for both molecular and histological purposes. The heart was removed via cardiectomy. Immediately after removal, the heart was cannulated via the aorta and flushed with cold Krebs-Henseleit Buffer. Once the heart was cleared, the cannula was removed in order to the record the weight of heart. The aorta was cannulated again and the bottom apical region of the heart was removed for molecular purposes, yielding left atrium, left ventricle, right atrium, and right ventricle tissue samples. The remaining upper portion of the heart was left intact and fixed via gravity perfusion fixation with 10% formalin at a mean arterial pressure of 100mmHg. Once the heart was fixed to satisfaction, they were cut on a short axis plane, starting at remaining apical region and continuing up to the base. The short axis sections were then cut in half, separating the heart into a lateral section and septal + RV section.

The tissue was then stored in 10% formalin until it underwent processing and was embedded in paraffin. Sections of the left atrium and right atrium were sectioned, processed and embedded in paraffin as well. For the lateral and septal sections of the left ventricle, 5µm tissue sections from 6 different levels from each sample were slide-mounted (AML Laboratories, Florida, USA).

Masson's Trichrome

Cytoplasm and muscle fibers stain red, while collagen (fibrosis) is stained blue. 120 slides (60 lateral wall, 60 septal wall) from 10 animals (sham=4, banded=6) and from 6 different levels of the LV were utilized to obtain representative data from different regions of the heart. A total of 1103 pictures were analyzed. The percentage of fibrotic tissue was determined as the collagen positive tissue out of the total stained LV tissue. For the left ventricle fibrotic gradient, the sub-endocardium and sub-epicardium were imaged separately. 20 slides (10 lateral wall, 10 septal wall) from 10 animals (sham=4, banded=6) were examined. A total of 267 pictures were analyzed for the LV fibrosis gradient. All images of the left ventricle were taken at 4x magnification (Nikon Eclipse Ni, NIS Elements software; New York, USA). For the left atrium, 40 slides from 10 animals (sham=4, banded=6) were examined and a total of 208 images were analyzed. All images were taken at 10x magnification. For the right atrium, 20 slides from 10 animals (sham=4, banded=6) were examined and a total of 204 images were analyzed. All images were taken at 10x magnification. For the right ventricle, 10 slides from 10 animals (sham=4, banded=6) were examined and a total of 208 images were analyzed. All images were taken at 20x magnification. All images were analyzed using Image J software with color

threshold analysis. The percentage of fibrotic tissue was determined as the collagen positive tissue out of the total stained LV tissue.

Cross-sectional Area

To examine myocyte cross-sectional area, LV tissue sections were stained for wheat germ agglutinin (WGA; Life Technologies; Eugene, OR) and nuclei were labeled with 4',6- diamidino-2-phenylindole (DAPI, Millipore; Billerica, MA). Images from all slides were acquired using a Nikon Eclipse T1 confocal microscope (Nikon Inc.; Mellvile, NY). All images were taken at 20x magnification. Myocyte cross-sectional area was measured using NIH Image J software as established previously[36]. A total of 6384 myocytes were counted from 15 animals (sham=7, banded=8). To examine a gradient in the cross-sectional area of left ventricle myocytes, the sub-endocardium and sub-epicardial layers were divided. A total of 8888 myocytes were counted, more specifically 4921 myocytes from the sub-endocardial layer and 3967 myocytes from the sub-epicardial layer, from 10 animals (sham=4, banded=6) animals were analyzed.

Statistics

Statistical analyses were completed using Graph Pad PRISM 6.07. Values are expressed as mean ± SEM, dependent variables were treated as being continuous, and a mixed-effects model was used. Variance multifactorial design and repeated measures on time were used to analyze ECHO and hemodynamic data (Time = baseline, 1, 2, 3, and 4-months post-surgery; treatment = sham vs. banded). Dunn-Bonferroni procedure was used to vertically compare treatment groups and compared to their baseline horizontally. The Mann-Whitney test was used for group comparisons. $p < 0.05$ was used as the cut off for accepting statistical significance.

CHAPTER 3

RESULTS

Confirmation of HFpEF Phenotype

Following the aortic banding or sham procedure, cats were followed out four-months post-banding. At no time point during the study were there any difference in body weight between sham and banded animals (Figure 3). At the end of the study, banded cats had significantly higher heart weight to body weight ratio compared to sham animals, which is an indicator for hypertrophy (Figure 3).

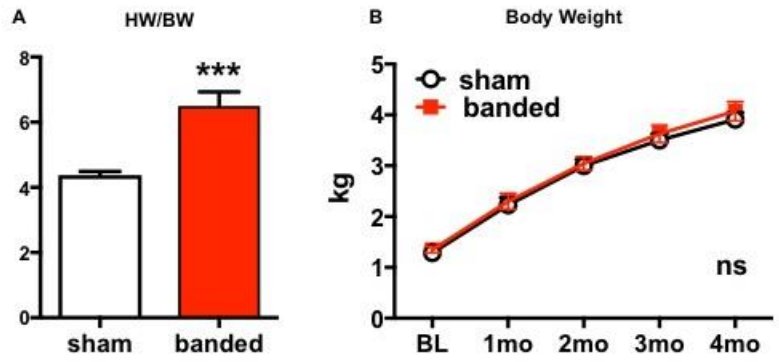

Figure 3. HW/BW ratio and Body Weight
(A) HW/BW ratio shows an increase in banded cats compared to sham cats. (B) No difference in body weight between banded cats compared to sham cats at any time point during the study. ***$p < 0.001$ between groups, † † † † <0.0001 vs BL. HW=heart weight, BW=body weight.

At baseline, there was no difference in NT-proBNP levels between banded and sham animals (banded: 35.4 ± 3.3pmol/L vs. sham: 42.1 ± 3.3pmol/L, $p = 0.99$), but there was a significant difference at four-months post banding (banded: 420.8 ± 179.9 pmol/L = 3566 ± 1270 pg/ml vs. sham: 26.1 ± 1.3 pmol/L = 221 ± 11 pg/ ml; $p < 0.01$) (Figure 4). Banded animals had significantly increased left ventricle wall thickness compared to sham animals at every time point after the aortic banding procedure (Figure 4).

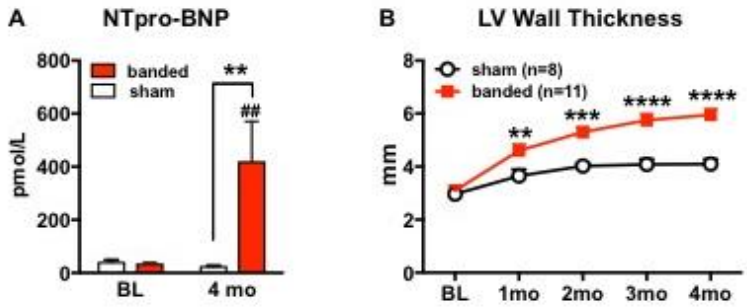

Figure 4. Changes in Myocardium
(A) NT-proBNP levels measured from serum at baseline and 4 months post-banding. (B) Banded cats had hypertrophy of the left ventricle as demonstrated in wall thickness. NT-proBNP=N-terminal pro-brain natriuretic peptide, LV Wall thickness=left ventricle wall thickness.

During terminal studies the pressure gradient across the band was measured invasively using fractional flow reserve (FFR) technique and the mean systolic pressure gradient was 52±12mmHg (Figure 5). The left ventricle end-diastolic pressure (LVEDP) was higher in banded cats compared to sham cats (Figure 5). There was no difference in left ventricle fractional shortening (LV FS) between the banded animals and sham animals, which is an assessment for systolic function. Left atrial end systolic volume was significantly different between banded animals and sham animals at every time point after baseline, and banded animals also had a significant increase within the group at each time point (LAV_{ES}: 1.05 ± 0.17 ml vs. 0.52 ± 0.04 ml at 4-months, $p < 0.001$). This functional data was previously described by our group[36].

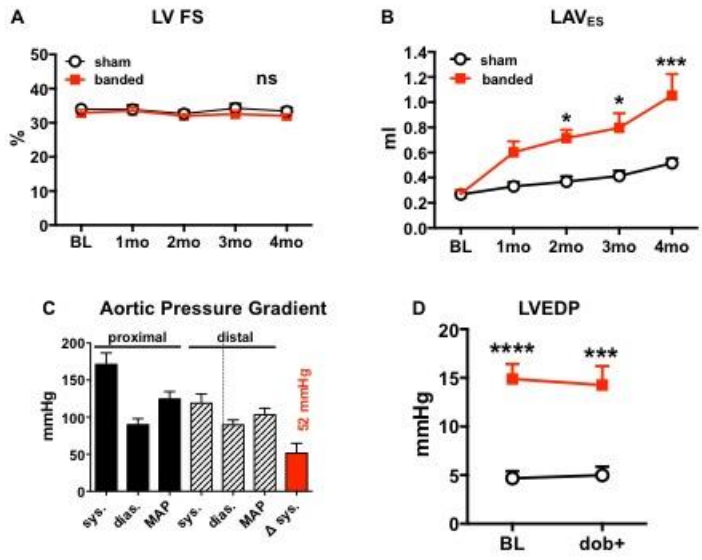

Figure 5. Confirmation of HFpEF phenotype
(A) LV FS displaying preserved systolic function in banded cats. (B) Left atrium was enlarged. (C) Pressure gradient across the band. (D) Banded cats had an increase in LVEDP. *p < 0.05, **p < 0.01, ***p < 0.001, ****p < 0.0001 between sham and banded animals. †p < 0.05, †††p < 0.001, ††††p < 0.0001 vs BL. LV FS= left ventricle fractional shortening, LAV_{ES}=left atrium end systolic volume, LVEDP=left ventricle end-diastolic pressure.

Fibrosis

Sections of the left atrium, left ventricle, right atrium, and right ventricle were stained with Masson's trichrome. The total percentage of aniline blue area (collagen) was calculated (Figure 6). When the total fibrotic area in the banded animals was compared to the sham animals, an increase was seen in the banded animals (banded: 8.4±1.6% vs sham: 4.0±0.3%; p<0.01). The lateral and septal walls of the left ventricle were then analyzed separately. Both of the walls showed an increase in fibrosis in banded compared to sham animals, but the difference was only significant in the lateral wall (banded: 10.2±2.2% vs sham: 3.6±0.2%, p<0.01).

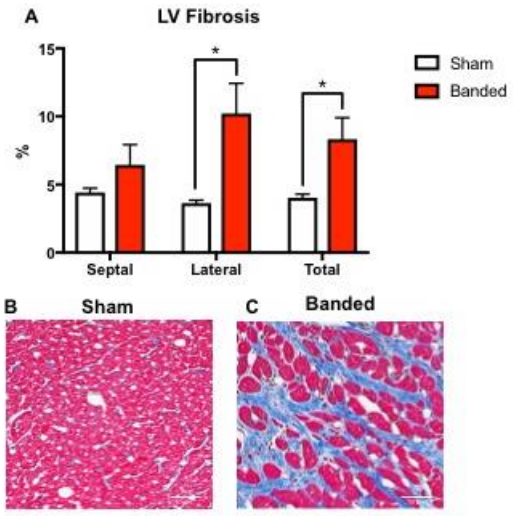

Figure 6. LV Fibrosis
(A) Quantification of LV fibrosis showed a significant increase in banded animals compared to sham animals. (B-C) Brightfield micrographs showing Masson's trichrome stained tissue sections in sham (B) vs. banded (C) animals. LV = left ventricle. Scale bar is 50μm.

In banded cats, the sub-endocardial layer had significantly more fibrosis compared to the sub-epicardial layer, forming a fibrotic gradient (Figure 7).

Figure 7. LV Fibrotic Gradient
(A) Quantification of LV fibrotic gradient showed a significant increase in the sub-endocardial layer compared to the sub-epicardial layer in banded animals. (B-C) Overview images of the LV and RV highlighting the difference in the fibrotic gradient between sham (B) and banded (C) animals. LV = left ventricle.

There was an increase in fibrosis in the left atrium in the banded animals compared to sham animals, but it was not significant (Figure 8).

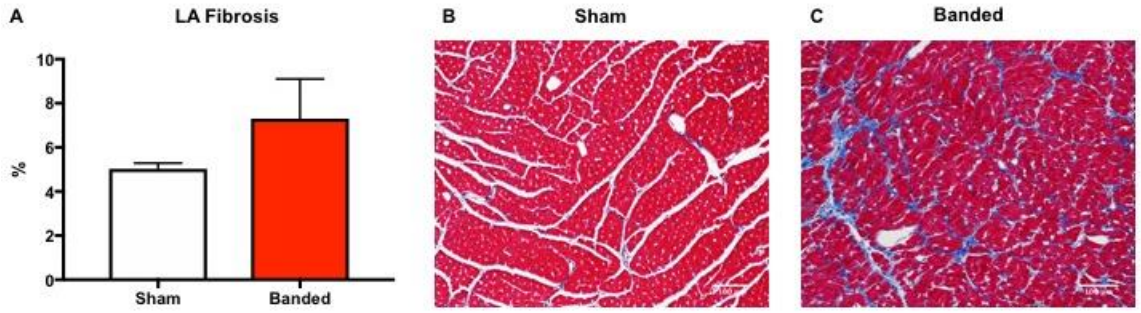

Figure 8. LA Fibrosis
(A) Quantification of LA fibrosis showed a slight increase in banded animals compared to sham animals. (B-C) Brightfield micrographs showing masson's trichrome stained tissue sections in sham (B) vs. banded (C) animals. LA = left atrium. Scale bar is 100µm.

There was a slight increase in fibrosis in the right atrium in banded cats compared to sham animals, but it was not significant (Figure 9).

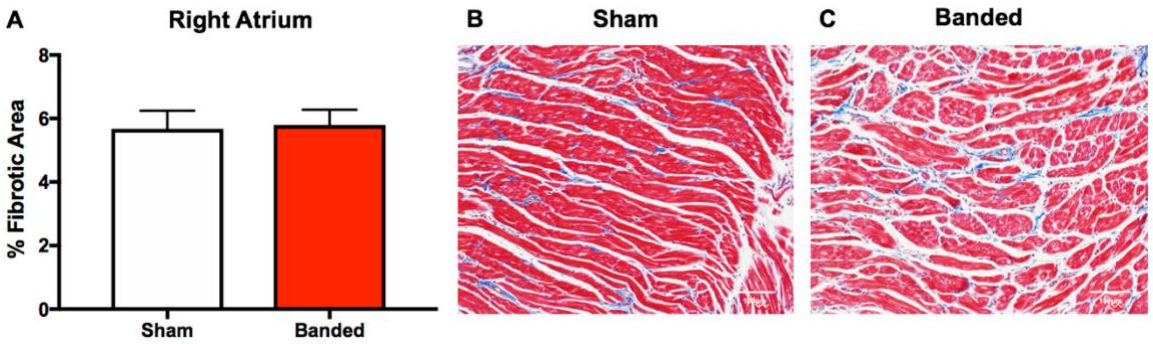

Figure 9. RA Fibrosis
(A) Quantification of RA fibrosis showed a slight increase in banded animals compared to sham animals. (B-C) Brightfield micrographs showing masson's trichrome stained tissue sections in sham (B) vs. banded (C) animals. RA = right atrium. Scale bar is 100μm.

There was also an increase in fibrosis in the right ventricle, but it was not significant (Figure 10).

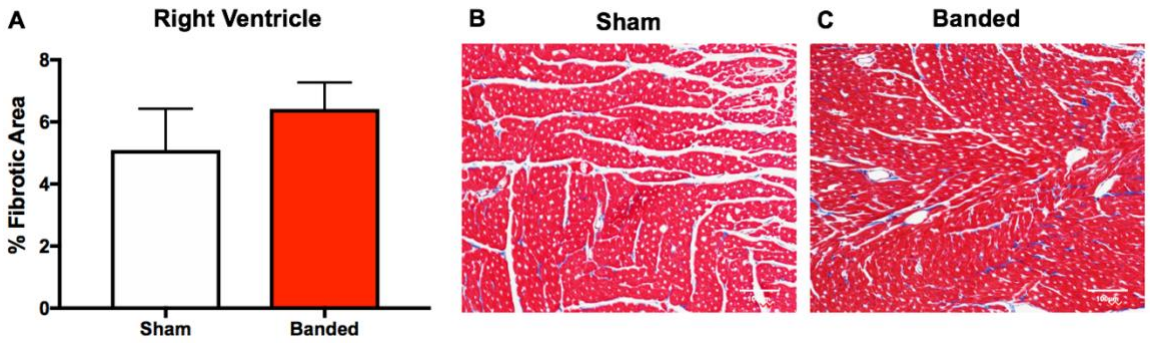

Figure 10. RV Fibrosis
(A) Quantification of RV fibrosis showed a slight increase in banded animals compared to sham animals. (B-C) Brightfield micrographs showing masson's trichrome stained tissue sections in sham (B) vs. banded (C) animals. RV = right ventricle. Scale bar = 100μm.

Cross-Sectional Area

Sections of the left ventricle were stained with wheat germ agglutinin (WGA), which labels cell membranes, in order to quantify cardiomyocyte cross-sectional area. The cross-sectional area of cardiomyocytes from banded animals was significantly larger compared to the sham animals ($468\pm24\mu m^2$ vs. $278\pm9\mu m^2$; $p<0.001$) (Figure 11). In banded animals, there was no gradient in cardiomyocyte size between the sub-endocardial layer and sub-epicardial layer (Figure 11). However, in sham animals the cross-sectional

area of sub-endocardial cardiomyocytes was increased compared to sub-epicardial myocytes (Figure 11).

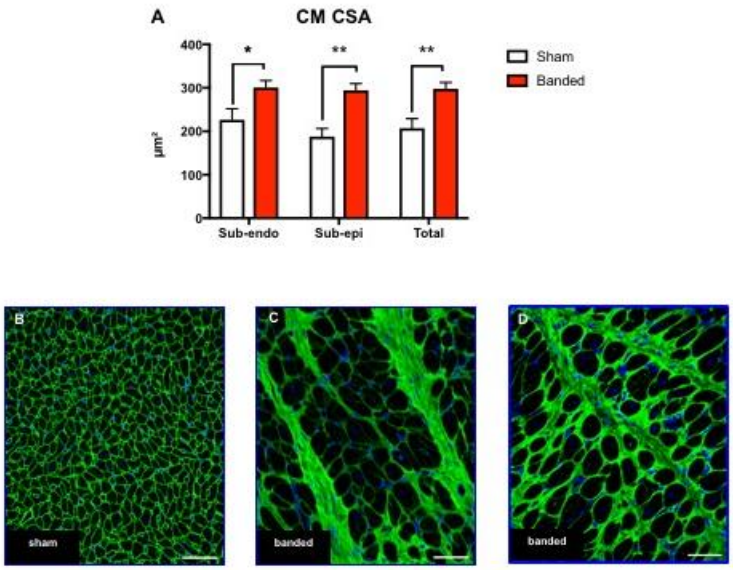

Figure 11. LV CM CSA
(A) Quantification of CM CSA showed a significant increase in CM size, indicating hypertrophy in banded animals compared to sham animals in the sub-endocardial layer, sub-epicardial layer, and total CSA. (B-D) Confocal micrographs of LV tissue sections stained for WGA (green) and DAPI (blue), which show an increase in CM size and extracellular matrix deposition in banded cats. LV = left ventricle, CM = cardiomyocyte, CSA = cross-sectional area. *$p < 0.05$, **$p < 0.01$. Scale bars = 50 µm.

CHAPTER 4

DISCUSSION

Other studies with large animal models of heart failure have examined fibrosis and hypertrophy, but we completed an in-depth analysis of the remodeling that takes place looking not only at fibrosis and hypertrophy in general, but also comparing the sub-endocardial to the sub-epicardial layer.

Aortic Banding

Four months post-aortic banding, we found that the banded animals had elevated left ventricle end-diastolic pressures, which is the gold standard for securing a HFpEF diagnosis [42]. Banded animals and sham animals had comparable NT-proBNP levels at baseline, but four months after aortic banding the banded animals had increased NT-proBNP levels compared to sham animals. The band created a pressure gradient and caused an increase in afterload, mimicking hypertension, which is the common risk factor for HFpEF [43]. ECHO based parameters of LV FS showed that the banded animals had no decrease in their global systolic function, but they did have left atrium enlargement and an increase in left ventricle wall thickness. While we have not quantified or defined signs and symptoms in our model, we have observed banded animals being less active than sham animals when they are housed together. Based off the functional data and the NT-proBNP, our model fits the guideline definition for a HFpEF diagnosis according to the European Society of Cardiology [6].

Fibrosis

The fibrosis present in HFpEF has been described as being interstitial, which is a reactive form of fibrosis[15]. Our histological analysis revealed an increase in fibrosis in the

left ventricle of banded animals compared to sham animals, which has been reported in other HFpEF animal models as well[44-46]. In the banded cats, we found more pronounced fibrosis in the lateral wall compared to the septal wall, which has not been reported elsewhere. This increase in fibrosis plays a role in the diastolic dysfunction[27] that we observed in our animals and the progression of the HFpEF phenotype. Interestingly, the fibrosis also formed a gradient from the sub-endocardial layer moving out to the sub-epicardial layer. Differences in the sub-endocardial layer and sub-epicardial layer were previously reported in a canine model of heart failure and left ventricle hypertrophy due to chronic-pressure overload, and examined in terms of limited sub-endocardial coronary reserve[47]. It has been established that following coronary artery occlusion, ischemic injury first occurs in the sub-endocardial layers and then moves out to sub-epicardial layer[48] and that sub-endocardial regions are more at risk during ischemic periods because they have a less blood supply than the sub-epicardium[49, 50]. A study by Vincent *et al.* concluded that severe valvular or supravalvular aortic stenosis can result in left ventricular sub-endocardial ischemia, ultimately resulting in under perfusion of the left ventricle sub-endocardial muscle in comparison to the oxygen demand[51]. Unverferth et al. stated that increased left-ventricular end-diastolic pressures produce a higher sub-endocardial resistance compared to sub-epicardial resistance to the diastolic coronary flow because the intraventricular pressure is primarily exerted on the sub-endocardium; they go on to state that the coronary reserve of the sub-endocardium is impaired and experiences an increase in the resistance to blood flow due to the increased filling pressures[52]. While making direct comparisons between our HFpEF model, aortic stenosis, and coronary artery occlusion would be inaccurate and inappropriate, the presentation of a fibrotic gradient does allow

for speculation. Perhaps the manifestation of the gradient is the result of slow, progressive ischemia due to hypoperfusion of the sub-endocardium, related to high LVEDPs. Since we use two-month old kittens for the aortic banding procedure, perhaps as they grow into the band slowly over the course of the four months post-banding the LVEDP continues to elevate, and the sub-endocardial layer becomes more oxygen deprived.

Hypertrophy

We clearly have cardiac hypertrophy occurring in the banded animals, as reflected by the increase in the HW/BW ratio. Upon further examination of the individual cardiomyocytes via immunohistochemistry, we found that we had an increase in cross-sectional area. Hypertrophy has been well documented in HFpEF [22, 43, 53] and has also been reported in other animal models[44, 46, 54]. While the findings for cardiomyocyte cross-sectional area were not novel, they do further support the HFpEF phenotype in this model. We also examined the cardiomyocyte cross-sectional area in terms of the sub-endocardial layer compared to the sub-epicardial layer. In banded animals, there was no difference between the sub-endocardial layer and sub-epicardial layer. In sham animals, the gradient between the sub-endocardial and sub-epicardial layers was significantly different. The cardiomyocyte cross-sectional area was larger in the sub-endocardial layer compared to the sub-epicardial layer. This observation has previously been described in the literature for normal, healthy rat and dog hearts [55, 56].

CHAPTER 5

CONCLUSIONS

This study has shown that a feline model of HFpEF has remodeling via fibrosis and hypertrophy. The fibrosis formed a gradient, starting in the sub-endocardial layer and decreasing outwards into the sub-epicardium. Banded animals also had cardiac hypertrophy, but there was no gradient in cardiomyocyte size between the sub-endocardium and sub-epicardium. All of the changes observed in the left ventricle contribute to the observed diastolic dysfunction and will serve as a baseline for remodeling as the study moves forward and looks at potential therapeutics.

Future Directions

Moving forward, the fibrotic gradient that we observed will be an interesting area for more research. Obviously, the fibrosis is a prime target for treatment as it is so profound in the banded cats compared the sham and its implications on the diastolic dysfunction are clear. Further examination into the differences between the lateral and septal wall fibrosis may provide insight into wall stress during HFpEF, but was outside the scope of this study.

Limitations

All animal models have limitations and our model is no exception. Recapitulating all of the complex risk factors and interacting pathophysiology that make up HFpEF is not an easy task. Since the aortic banding is the sole cause of the slow-progressive pressure over-load in the kittens and there are no other comorbidities, such as obesity, diabetes, or systemic hypertension, we are really only capturing one aspect of the disease. The kittens are also young during the study and we perform terminal studies at 4 months post banding, so any changes that occur after that point are unknown. We also have no way of tracking

the progression of fibrosis or hypertrophy throughout the study since we only do tissue harvest at 4 months post-banding. Preliminary experiments were performed in both male and female kittens, but the female cats developed a less severe phenotype. In order to develop a more severe phenotype, only male kittens were used.

REFERNCES:

1. What is heart failure?

2. Heidenreich PA, Albert NM, Allen LA, Bluemke DA, Butler J, Fonarow GC, Ikonomidis JS, Khavjou O, Konstam MA, Maddox TM, Nichol G, Pham M, Piña IL, Trogdon JG, Committee AHAAC, Council on Arteriosclerosis TraVB, Intervention CoCRa, Cardiology CoC, Prevention CoEa, Council S. Forecasting the impact of heart failure in the united states: A policy statement from the american heart association. *Circ Heart Fail*. 2013;6:606-619

3. Ziaeian B, Fonarow GC. Epidemiology and aetiology of heart failure. *Nat Rev Cardiol*. 2016;13:368-378

4. Cook C, Cole G, Asaria P, Jabbour R, Francis DP. The annual global economic burden of heart failure. *Int J Cardiol*. 2014;171:368-376

5. Bhuiyan T, Maurer MS. Heart failure with preserved ejection fraction: Persistent diagnosis, therapeutic enigma. *Curr Cardiovasc Risk Rep*. 2011;5:440-449

6. Ponikowski P, Voors AA, Anker SD, Bueno H, Cleland JG, Coats AJ, Falk V, González-Juanatey JR, Harjola VP, Jankowska EA, Jessup M, Linde C, Nihoyannopoulos P, Parissis JT, Pieske B, Riley JP, Rosano GM, Ruilope LM, Ruschitzka F, Rutten FH, van der Meer P. 2016 esc guidelines for the diagnosis and treatment of acute and chronic heart failure. *Rev Esp Cardiol (Engl Ed)*. 2016;69:1167

7. Little WC, Zile MR. Hfpef: Cardiovascular abnormalities not just comorbidities. *Circ Heart Fail*. 2012;5:669-671

8. Lam CS, Solomon SD. The middle child in heart failure: Heart failure with mid-range ejection fraction (40-50%). *Eur J Heart Fail*. 2014;16:1049-1055

9. Oktay AA, Rich JD, Shah SJ. The emerging epidemic of heart failure with preserved ejection fraction. *Curr Heart Fail Rep*. 2013;10:401-410

10. Sharma K, Kass DA. Heart failure with preserved ejection fraction: Mechanisms, clinical features, and therapies. *Circ Res*. 2014;115:79-96

11. Quiñones MA, Zile MR, Massie BM, Kass DA, Discourses WCotDD. Chronic heart failure: A report from the dartmouth diastole discourses. *Congest Heart Fail*. 2006;12:162-165

12. Jessup M, Abraham WT, Casey DE, Feldman AM, Francis GS, Ganiats TG, Konstam MA, Mancini DM, Rahko PS, Silver MA, Stevenson LW, Yancy CW. 2009 focused update: Accf/aha guidelines for the diagnosis and management of heart failure in adults: A report of the american college of cardiology foundation/american heart association task force on practice guidelines: Developed in collaboration with the international society for heart and lung transplantation. *Circulation*. 2009;119:1977-2016

13. Reddy YN, Borlaug BA. Heart failure with preserved ejection fraction. *Curr Probl Cardiol*. 2016;41:145-188

14. Dunlay SM, Roger VL, Redfield MM. Epidemiology of heart failure with preserved ejection fraction. *Nat Rev Cardiol*. 2017;14:591-602

15. van Heerebeek L, Paulus WJ. Understanding heart failure with preserved ejection fraction: Where are we today? *Neth Heart J*. 2016;24:227-236

16. Martin M. LeWinter M, Markus Meyer M. Mechanisms of diastolic dysfunction in hfpef: If it's not one thing it's another *Circulation Heart Failure*. 2013;6:1112–1115

17. Dick SA, Epelman S. Chronic heart failure and inflammation: What do we really know? *Circ Res*. 2016;119:159-176

18. Medicine USNLo. National institute of health.

19. Lekavich CL, Barksdale DJ, Neelon V, Wu JR. Heart failure preserved ejection fraction (hfpef): An integrated and strategic review. *Heart Fail Rev*. 2015;20:643-653

20. Franssen C, González Miqueo A. The role of titin and extracellular matrix remodelling in heart failure with preserved ejection fraction. *Neth Heart J*. 2016;24:259-267

21. Frey N, Katus HA, Olson EN, Hill JA. Hypertrophy of the heart: A new therapeutic target? *Circulation*. 2004;109:1580-1589

22. Borlaug BA. The pathophysiology of heart failure with preserved ejection fraction. *Nat Rev Cardiol*. 2014;11:507-515

23. Krenning G, Zeisberg EM, Kalluri R. The origin of fibroblasts and mechanism of cardiac fibrosis. *J Cell Physiol*. 2010;225:631-637

24. Zile MR, Baicu CF, Ikonomidis JS, Stroud RE, Nietert PJ, Bradshaw AD, Slater R, Palmer BM, Van Buren P, Meyer M, Redfield MM, Bull DA, Granzier HL, LeWinter MM. Myocardial stiffness in patients with heart failure and a preserved ejection fraction: Contributions of collagen and titin. *Circulation*. 2015;131:1247-1259

25. Shah SJ, Kitzman DW, Borlaug BA, van Heerebeek L, Zile MR, Kass DA, Paulus WJ. Phenotype-specific treatment of heart failure with preserved ejection fraction: A multiorgan roadmap. *Circulation*. 2016;134:73-90

26. Burchfield JS, Xie M, Hill JA. Pathological ventricular remodeling: Mechanisms: Part 1 of 2. *Circulation*. 2013;128:388-400

27. Rockey DC, Bell PD, Hill JA. Fibrosis--a common pathway to organ injury and failure. *N Engl J Med*. 2015;373:96

28. Dobaczewski M, Chen W, Frangogiannis NG. Transforming growth factor (tgf)-β signaling in cardiac remodeling. *J Mol Cell Cardiol*. 2011;51:600-606

29. Kong P, Christia P, Frangogiannis NG. The pathogenesis of cardiac fibrosis. *Cell Mol Life Sci*. 2014;71:549-574

30. Leonard BL, Smaill BH, LeGrice IJ. Structural remodeling and mechanical function in heart failure. *Microsc Microanal*. 2012;18:50-67

31. Chien KR, Zhu H, Knowlton KU, Miller-Hance W, van-Bilsen M, O'Brien TX, Evans SM. Transcriptional regulation during cardiac growth and development. *Annu Rev Physiol*. 1993;55:77-95

32. Hunter JJ, Chien KR. Signaling pathways for cardiac hypertrophy and failure. *N Engl J Med*. 1999;341:1276-1283

33. Doust J, Lehman R, Glasziou P. The role of bnp testing in heart failure. *Am Fam Physician*. 2006;74:1893-1898

34. Wong PC, Guo J, Zhang A. The renal and cardiovascular effects of natriuretic peptides. *Adv Physiol Educ*. 2017;41:179-185

35. Bay M, Kirk V, Parner J, Hassager C, Nielsen H, Krogsgaard K, Trawinski J, Boesgaard S, Aldershvile J. Nt-probnp: A new diagnostic screening tool to differentiate between patients with normal and reduced left ventricular systolic function. *Heart*. 2003;89:150-154

36. Wallner M, Eaton DM, Berretta RM, Borghetti G, Wu J, Baker ST, Feldsott EA, Sharp TE, Mohsin S, Oyama MA, von Lewinski D, Post H, Wolfson MR, Houser SR.

A feline hfpef model with pulmonary hypertension and compromised pulmonary function. *Sci Rep*. 2017;7:16587

37. Kitzman DW. Understanding results of trials in heart failure with preserved ejection fraction: Remembering forgotten lessons and enduring principles. *J Am Coll Cardiol*. 2011;57:1687-1689

38. Bailey BA, Houser SR. Sarcoplasmic reticulum-related changes in cytosolic calcium in pressure-overload-induced feline lv hypertrophy. *Am J Physiol*. 1993;265:H2009-2016

39. Pollack PS, Bailey BA, Budjak R, Fernandez E, Houser SR. Progressive feline pressure-overload: Noninvasive assessment correlates with abnormalities in single cells. *Am J Physiol*. 1993;264:H1307-1314

40. Bailey BA, Dipla K, Li S, Houser SR. Cellular basis of contractile derangements of hypertrophied feline ventricular myocytes. *J Mol Cell Cardiol*. 1997;29:1823-1835

41. Bailey BA, Houser SR. Calcium transients in feline left ventricular myocytes with hypertrophy induced by slow progressive pressure overload. *J Mol Cell Cardiol*. 1992;24:365-373

42. Huis In 't Veld AE, de Man FS, van Rossum AC, Handoko ML. How to diagnose heart failure with preserved ejection fraction: The value of invasive stress testing. *Neth Heart J*. 2016;24:244-251

43. Borlaug BA, Paulus WJ. Heart failure with preserved ejection fraction: Pathophysiology, diagnosis, and treatment. *Eur Heart J*. 2011;32:670-679

44. Regan JA, Mauro AG, Carbone S, Marchetti C, Gill R, Mezzaroma E, Valle Raleigh J, Salloum FN, Van Tassell BW, Abbate A, Toldo S. A mouse model of heart failure with preserved ejection fraction due to chronic infusion of a low subpressor dose of angiotensin ii. *Am J Physiol Heart Circ Physiol*. 2015;309:H771-778

45. Gallet R, de Couto G, Simsolo E, Valle J, Sun B, Liu W, Tseliou E, Zile MR, Marbán E. Cardiosphere-derived cells reverse heart failure with preserved ejection fraction (hfpef) in rats by decreasing fibrosis and inflammation. *JACC Basic Transl Sci*. 2016;1:14-28

46. Zakeri R, Moulay G, Chai Q, Ogut O, Hussain S, Takahama H, Lu T, Wang XL, Linke WA, Lee HC, Redfield MM. Left atrial remodeling and atrioventricular coupling in a canine model of early heart failure with preserved ejection fraction. *Circ Heart Fail*. 2016;9

47. Hittinger L, Shannon RP, Bishop SP, Gelpi RJ, Vatner SF. Subendomyocardial exhaustion of blood flow reserve and increased fibrosis in conscious dogs with heart failure. *Circ Res*. 1989;65:971-980

48. Khokhlova A, Iribe G, Yamaguchi Y, Naruse K, Solovyova O. Effects of simulated ischemia on the transmural differences in the frank-starling relationship in isolated mouse ventricular cardiomyocytes. *Prog Biophys Mol Biol*. 2017

49. Algranati D, Kassab GS, Lanir Y. Why is the subendocardium more vulnerable to ischemia? A new paradigm. *Am J Physiol Heart Circ Physiol*. 2011;300:H1090-1100

50. Toyota E, Ogasawara Y, Hiramatsu O, Tachibana H, Kajiya F, Yamamori S, Chilian WM. Dynamics of flow velocities in endocardial and epicardial coronary arterioles. *Am J Physiol Heart Circ Physiol*. 2005;288:H1598-1603

51. Vincent WR, Buckberg GD, Hoffman JI. Left ventricular subendocardial ischemia in severe valvar and supravalvar aortic stenosis. A common mechanism. *Circulation*. 1974;49:326-333

52. Unverferth DV, Magorien RD, Lewis RP, Leier CV. The role of subendocardial ischemia in perpetuating myocardial failure in patients with nonischemic congestive cardiomyopathy. *Am Heart J*. 1983;105:176-179

53. Rose-Jones LJ, Rommel JJ, Chang PP. Heart failure with preserved ejection fraction: An ongoing enigma. *Cardiol Clin*. 2014;32:151-161, ix-x

54. Methawasin M, Strom JG, Slater RE, Fernandez V, Saripalli C, Granzier H. Experimentally increasing the compliance of titin through rna binding motif-20 (rbm20) inhibition improves diastolic function in a mouse model of heart failure with preserved ejection fraction. *Circulation*. 2016;134:1085-1099

55. Gerdes AM, Callas G, Kasten FH. Differences in regional capillary distribution and myocyte sizes in normal and hypertrophic rat hearts. *Am J Anat*. 1979;156:523-531

56. Gerdes AM, Kasten FH. Morphometric study of endomyocardium and epimyocardium of the left ventricle in adult dogs. *Am J Anat*. 1980;159:389-394